

Environmental Science Center, Peking University, Beijing 100781, P.R. of China

## Persistent high concentration of ozone during windstorm conditions in southern Korea

H. Choi

With 19 Figures

Received April 16, 2003; revised July 10, 2003; accepted August 29, 2003

Published online: June 2, 2004 © Springer-Verlag 2004

### Summary

Prior to and following the development of a windstorm in the mountainous coastal area of southern Korea, ground level ozone ( $O_3$ ) concentrations near Kangnung city, on the lee side of the mountains, show a maximum value at approximately 1300 LST, owing to a photolytic cycle of  $NO_2$ – $NO$ – $O_3$  during the day and a minimum in concentrations at night as a result of the reverse cycle. During the development period of the windstorm, ozone concentrations are generally high all day, and slightly higher during the night. This distribution pattern of ozone is very different from the typical distribution of ozone in the absence of windstorms. High daytime concentrations of ozone during the windstorm are due to both the increase in the amount of ozone from photochemical reactions involving  $NO_x$  and the increase in  $O_3$  concentration due to a decrease in the convective boundary layer thickness under the influence of downslope windstorm conditions on the lee-side of the mountains. At night, the windstorm increases in intensity as the westerly winds combine with a katabatic wind blowing downslope toward the surface at the coast. This causes momentum transport of air parcels in the upper levels toward the surface at the coast and the development of internal gravity waves, which generate a hydraulic jump directed upward over the coast and the East sea, thereby reducing to very thin the thickness of the nocturnal surface inversion layer (NSIL). The higher  $O_3$  concentration at night depends mainly upon the shallow NSIL and on some  $O_3$  being transported by the momentum transfer from the upper troposphere toward the ground in windstorm conditions.

### 1. Introduction

Variations in  $O_3$  concentration during a windstorm and sea-land breeze circulations in the mountainous coastal region of southern Korea are complex, especially compared to the typical pattern of ozone variation in spring. In recent years, the interpretation of daily and seasonal variations in the amount of surface ozone has been undertaken by considering the influence of various meteorological phenomena and chemical reactions (Evan et al, 1983; Hales, 1996). Tropospheric ozone originates from two sources, namely, the formation from chemical processes among tropospheric trace gases and from the transport of intermittent stratospheric ozone into the troposphere (Jacob, 1999). Pazenny and Brasseur (1997) and McKee (1994) pointed out that the most important tropospheric ozone precursors were nitrogen oxides ( $NO_x = NO + NO_2$ ), carbon monoxide (CO), methane ( $CH_4$ ) and other non-methanes.

Baird (1995) indicated that oxidation also can react to convert NO to  $NO_2$  via the ozone forming process and more than one NO-molecule must be oxidized to  $NO_2$  per hydrocarbon molecule broken up, in order to permit ozone

to accumulate during the day. Kimura (1983) explained that as the nitric oxide was oxidized to nitrogen dioxide through the reaction of the hydrocarbons, urban ozone could build up to a maximum concentration close to 1300 LST and a minimum concentration at night. All these precursors are products of fossil fuel and biomass burning, and the increase of ozone in near-surface air is mainly the result of increased  $\text{NO}_x$ -emissions.

The transport of chemical species between stratosphere and troposphere may also play an important role in the atmospheric chemistry near the surface. Girdzine (1991) explained that the highest ozone concentrations in Lithuania were connected with an efficient stratosphere-troposphere exchange as measured by surface ozone. For the enhancement of ozone in the troposphere from the stratosphere, downward transport from the stratosphere presents a significant source of tropospheric ozone and constitutes the ultimate removal mechanism for many stratospheric species such as ozone depletion (Austin and Midgley, 1994; Moon et al, 2002; Seinfeld and Pandis, 1998). Stratosphere-troposphere exchange is associated with weather conditions such as tropopause folding in the rear of an upper level jet streak, in cut-off lows in mid-latitudes and surface high-pressure systems (Cooper et al, 1998; Davis and Schuepbach, 1994; Kondratyev and Varotsos, 2000; Kim et al, 2002).

Previous studies on ozone concentration near the surface indicate a maximum value at about noon and a minimum at night. Observations of ozone concentration in this study presented a very different pattern of ozone concentration during windstorm conditions. Prior to and following a windstorm in the mountainous coastal area, surface ozone concentrations near the coast on the lee side reach a maximum value at approximately 1300 LST, during the day and a minimum at night. On the other hand,  $\text{O}_3$  concentrations in daylight hours during the windstorm are much higher than in non-windstorm conditions, and the concentrations are slightly higher at night than during the day.

In this paper, some possible mechanisms are proposed for the occurrence of high concentrations of ground level ozone in the mountainous coastal area. What are the meteorological conditions that result in the enhancement of ozone,

both during the day and at night? What are the important driving mechanisms for the high concentration of ozone during windstorms? To answer these questions analysis of the synoptic-, meso- and micro-scale meteorology using vertical cross-sections of meteorological elements, such as wind and potential temperature, are essential for understanding the exchange and advection of ozone and other gases that enhance ozone concentrations near the coastal surface on the lee side of the mountains.

## 2. Data collection

### 2.1 Topographic feature near sampling site

Figure 1 shows the topographical features and air quality monitoring sites in the study area. The two monitoring sites of Kangnung and Wonju are located near the coast and inland, respectively. Local land-sea circulations affect the air quality in the two cities. In the study area around Kangnung city, shown in the fine-mesh domain (Fig. 1b), there are contrasting features that consist of an inland plain, high mountains, a narrow inland basin and the adjacent sea. Kangnung city located in the narrow coastal basin has no significant pollution sources. Wonju city, situated west of Mt. Taegulyang and 100 km from Kangnung city, was selected for verification of the advection of ozone into Kangnung city. In the coarse-mesh domain, the Tae Bak mountains are oriented north-south along the east coast of Korea and another branch stretches toward the south-west (Fig. 1). The study area in the fine-mesh domain consists of complex terrain characterized by forest on high, steep sloping mountains in the west, Kangnung city on the narrow, central plain and sea to the east. The climate of this area is generally affected both by land and sea. As a consequence, synoptic-scale westerly or easterly winds, meso-scale sea or land breezes and local mountain-valley winds frequently interact with each other resulting in complex wind patterns.

### 2.2 Data acquisition

Hourly data of  $\text{O}_3$  concentration from 0100 LST on March 26 to 2400 LST on March 29, 1994

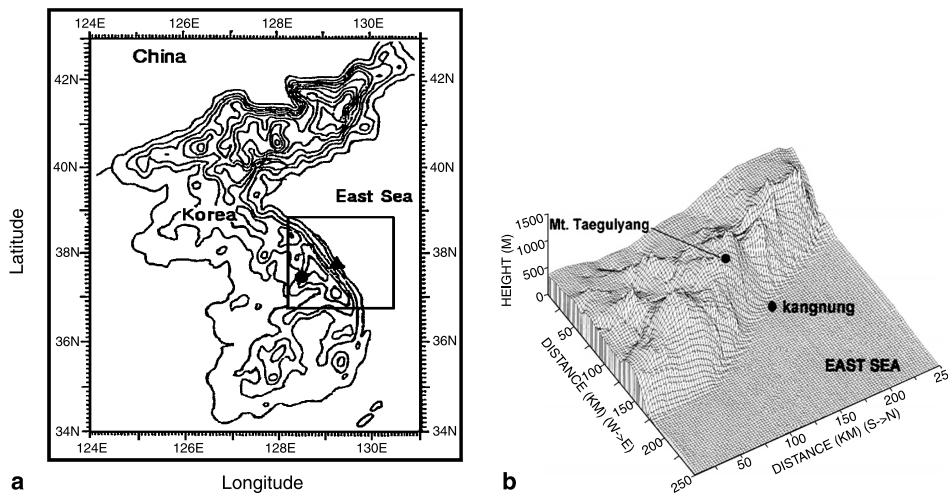


**Fig. 1a.** Nested grid system with the box indicating the fine-mesh domain used for the meteorological model simulation. The black coloured triangle and circle denote Kangnung city and Wonju city, respectively; **b** Fine mesh domain showing Mt. Taegulyang (865 m) in the Tae Bak mountains along the east coast, to the west of Kangnung city

were measured automatically by an ozone analyzer (DASBI-1108) and  $\text{NO}_x$  concentrations were also measured using an analyzer (DASBI-2108). These instruments were positioned on the top of the Imdangdong Administration Office building in downtown Kangnung city at a height of 10 metres above mean sea level. The accuracy of the models was consistent over the period that the air quality measurements were considered. As this monitoring site is located near the centre of the coastal city of Kangnung, the air quality can be affected by both emission inventories such as fuel combustion of vehicle and gas boilers in residential areas and also local atmospheric circulations due to the proximity of high topography and adjacent sea.

Another sampling site in Wonju city is located in the western basin about 100 km away from Kangnung city, where the Wonju Regional Environmental Administration, Ministry of Environment of Korean Government (WREA, 1994) automatically reanalyzes measured air quality data. The detectors measure the concentrations of  $\text{NO}_x$  and  $\text{NO}_2$ , and the difference between the two measurements should be regarded as the concentration of NO.

### 2.3 Numerical model and input data

A three-dimensional non-hydrostatic grid point model called LAS-V, using a one way double nesting in a terrain following coordinate system

$(x, y, z^*)$ , was originally developed by the Meteorological Research Institute (MRI), Japan Meteorological Agency (JMA). This system was adopted for this study to investigate the structure of windstorm conditions and to simulate the large scale atmospheric circulation in north eastern Asia, and local scale circulations in the mountainous coastal region. The model was run from 0900 LST, March 27 to 1200 LST, March 28, consisting of forecasts out to 30 hours on a Hitachi super computer at MRI (Takahashi, 1997).

The model domain consists of  $34 \times 34$  grid points with a uniform horizontal interval in the 20 km and 7 km coarse-mesh and fine-mesh domains, respectively, and 16 vertical levels between 10 m and 6 km at increasingly larger intervals with height. Twelve hourly global analysis data (G-ANAL) at  $1.25^\circ$  resolution including pressure, wind, potential temperature and specific humidity on five levels from the surface to 100 hPa were generated at JMA and were horizontally and vertically interpolated to the coarse-mesh domain as input data. Simulated values from the three-dimensional hydrostatic model were input as lateral boundary conditions for running the non-hydrostatic model over the fine-mesh domain. Sea-surface temperature data derived from NOAA satellite images by the National Fisheries and Development Agency were also used as model input data for the two domains (NFRDA, 1994).

### 3. Results

#### 3.1 Ozone concentration and occurrence of windstorm conditions

Figures 2 and 3 show the temporal distribution of surface ozone and nitrogen dioxide measured by  $O_3$  and  $NO_x$  analyzers near the centre of Kangnung city. In this study, the research period was classified into two categories consisting of windstorm conditions and without windstorm conditions. Prior to 2200 LST, March 26, the surface wind speed in the city was very light (less than  $3 \text{ m s}^{-1}$ ) and after 2200 LST it gradually increased (Fig. 4). After 0600 LST, March 27, a strong surface wind greater than  $5 \text{ m s}^{-1}$  continued in the Kangnung coastal region and reached windstorm speed (greater than  $10 \text{ m s}^{-1}$ ). The centre of the windstorm reached a maximum speed of  $25 \text{ m s}^{-1}$  (Fig. 9), persisted in the coastal region until midnight on March 28, and the wind speed near the surface was greater

than  $10 \text{ m s}^{-1}$ . Then, as the windstorm disappeared on March 29, the strong wind speeds decreased to very light.

On March 26 and March 29, prior to and following the windstorm,  $O_3$  concentrations at the surface in Kangnung city showed a typical urban pattern with a maximum value near noon and a minimum at night. When the  $O_3$  concentration decreased during the afternoon of March 26,  $NO_2$  concentration increased. From 2000 LST to midnight,  $NO_2$  concentration rapidly decreased, becoming very low before sunrise (Fig. 2).  $NO$  concentration showed a similar pattern to  $NO_2$  concentration, which greatly influenced the  $NO_x$  concentration (Fig. 3).

Kangnung has very clean air with no factories. Emission sources are confined to fuel combustion from vehicles and residential gas boilers. As nitric oxide was oxidized to nitrogen dioxide through the reaction of the hydrocarbons, for example, during the photolytic cycle of  $NO-NO_2-O_3$ , the ozone at Kangnung city increased,

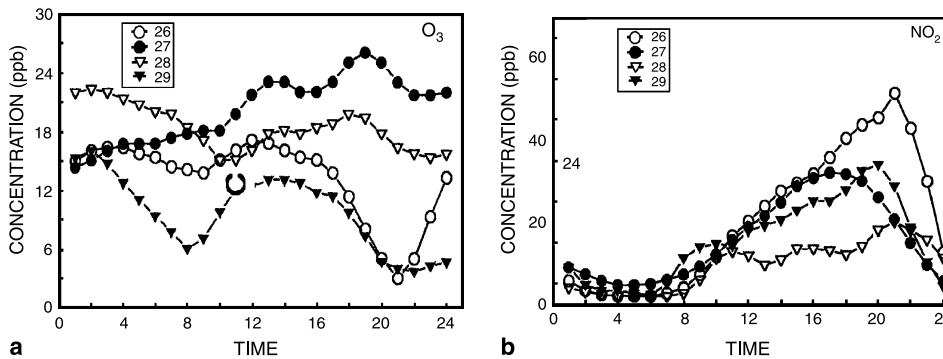


**Fig. 2.** Hourly concentrations of  $O_3$  (ppb) and  $NO_2$  (ppb) at Kangnung city from March 26 through March 29, 1994. The wind speed on March 26 was moderate. Windstorm conditions lasted from the evening of March 26 until midnight on March 28

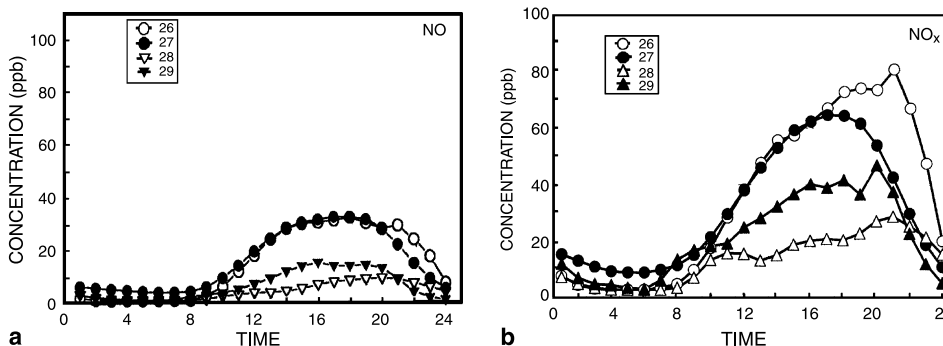


**Fig. 3.** As shown in Fig. 2, except for  $NO$  (ppb) and  $NO_x$  (ppb) at Kangnung city from March 26 through 29, 1994

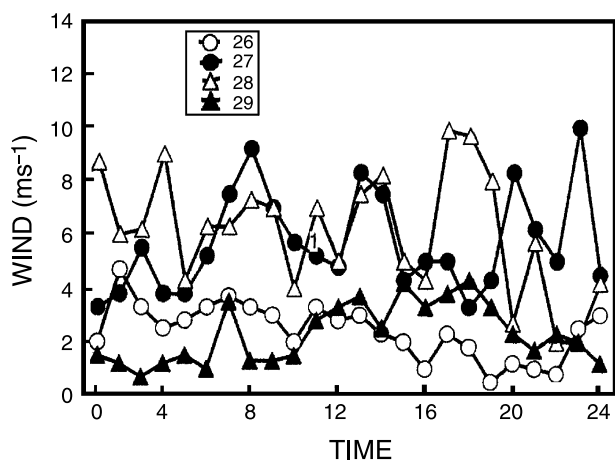


**Fig. 4.** Hourly distribution of observed wind speeds ( $\text{m s}^{-1}$ ) at Kangnung city from March 26 through March 29, 1994. Note the strong wind speeds from the evening of March 26 to midnight on March 28 and weak wind speeds on March 26 and again on March 29

reaching a maximum concentration at approximately 1300 LST. Low concentrations of  $\text{O}_3$  during the night are due to the fact that there is no photochemically produced  $\text{O}_3$ , but there are processes that destroy  $\text{O}_3$  based on the reaction of  $\text{NO}_2$  with  $\text{O}_3$ . Mainly high concentrations of  $\text{O}_3$  during the day are attributed to the photochemical reaction of  $\text{NO}_2$  into  $\text{O}_3$ , which is well known (Hobbs, 2000). Although it is known that the increase of ozone in the near-surface air in an urban area is mainly produced as a result of increased  $\text{NO}_x$ -emissions, it is very difficult to attribute an increase to that cause during a windstorm.

For example, hourly variations of both  $\text{NO}_2$  and  $\text{NO}$  on March 26 and March 27 are similar, but daytime surface ozone concentrations on March 27 during the windstorm were much higher than on March 26. In general, nighttime surface ozone concentration decreased rapidly after sunset, but on March 27 it also increased during nighttime hours, with a maximum concentration at 1900 LST. Daytime ozone concentration during the windstorm was also much higher than in the absence of the windstorm. Moreover, nighttime ozone concentration during the windstorm did not decrease, but rather increased all night, when it reached its maximum concentration.

It is necessary to investigate why  $\text{O}_3$  concentrations on March 27 during the windstorm were

very high, throughout the day and even higher during the night. The first step was to investigate the photochemical reaction cycle of  $\text{NO}-\text{NO}_2-\text{O}_3$ . The weather on March 26, before the windstorm, was dry on the coast at Kangnung and a typical photochemical reaction process including the destruction of  $\text{O}_3$  in the  $\text{NO}-\text{NO}_2-\text{O}_3$  cycle was expected to occur both during the day and night.

As the weather on March 27 during the windstorm and on March 26, the day before the windstorm, was also dry, there was no doubt that photochemical production of  $\text{O}_3$  from  $\text{NO}_x$  was occurring during the day, because a high concentration of ozone was still found at 1300 LST when it was mainly due to photochemical activity.  $\text{NO}_2$  concentrations during the day on March 26 in the absence of windstorm conditions were almost the same as on March 27 during the windstorm, but  $\text{O}_3$  concentration on March 27 was approximately twice as high as on March 26. Even though the weather on both days was dry and almost same amount of  $\text{O}_3$  could be photochemically produced from  $\text{NO}_2$ , the resulting concentration of ozone was quite different. Therefore, ascertaining the mechanism on both days, for the occurrence of high ozone concentration, is essential.

The second step is to understand how weather conditions can affect the enhancement of daytime ozone concentration during a windstorm and in the absence of a windstorm system. Figure 5 shows that high pressure, with central value 1032 hPa at 1500 LST, March 27, was approaching the southern part of the Korean peninsula. The resulting weather on the Kangnung coast was fine with a south-westerly wind greater than  $5 \text{ m s}^{-1}$ . Near a height of 4 km, a north-westerly wind greater than  $20 \text{ m s}^{-1}$  dominated the study area (Fig. 9).

Seinfeld and Pandis (1998) indicated that since a high-pressure weather system is characterized by widespread sinking motion through most of troposphere, peak concentrations of ozone could occur due to both transport from upper tropospheric levels and catalytic chemical reactions, when solar radiation was high and air temperatures became higher than those of the day before. For example, on March 27, a high pressure system was responsible for fine weather in the study area and the vertical profile of wind speed

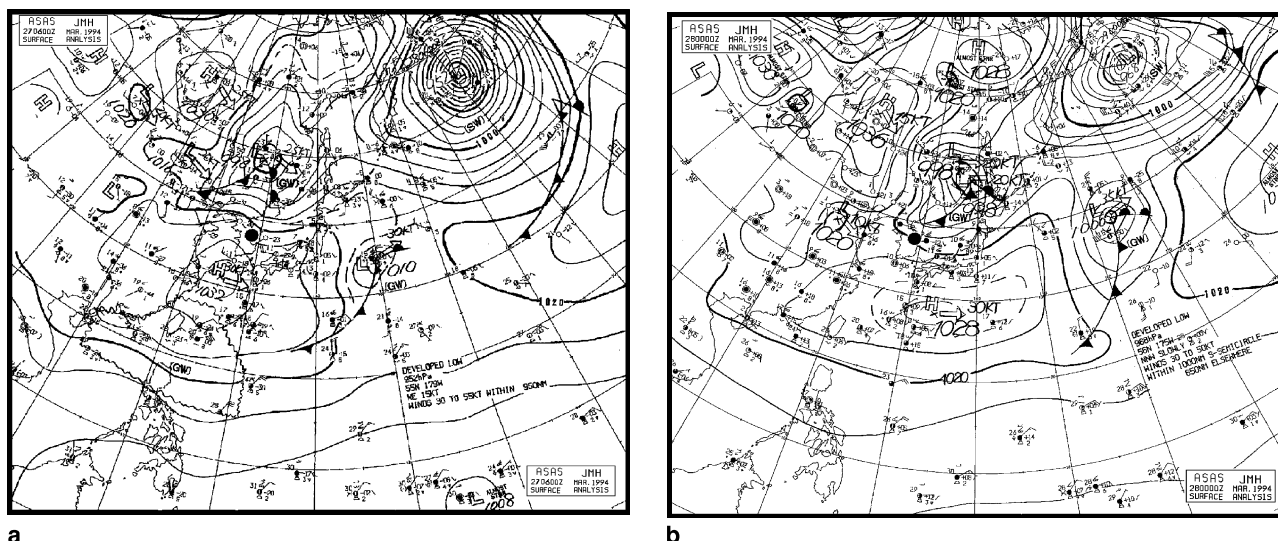


**Fig. 5.** MSLP charts at, (a) 1500 LST (0600 UTC), 27 March, 1994, and (b) 0900 LST (0000 UTC), March 28, 1994. Solid black circle in the central part of the map denotes the study area in Korea

gradually decreased from a height of 10,000 m to the surface (Figs. 7 and 17). Hence, some ozone may be transported from high in the troposphere due to subsidence and enhance the ozone concentration at the surface.

In this study, daytime air temperatures during the windstorm period of March 27 and 28, when high surface concentrations of ozone occurred, were 3 °C or 7 °C higher than on March 26 and March 29 in the absence of windstorm conditions. Moreover, on March 27, high-pressure extended over the study region and the air temperature was higher than the day before (as shown in Fig. 6), so that the weather could have contributed to the increase in surface ozone in the study area.

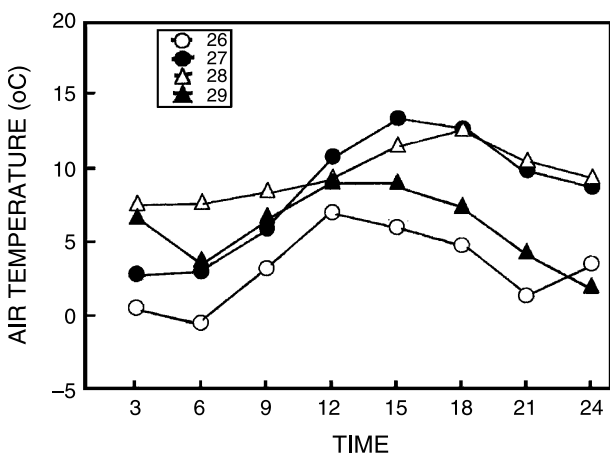


**Fig. 6.** Air temperature (°C) every three hours at Kangnung city from March 26 through 29, 1994

At 0900 LST, March 28 (the next morning), the weather in the study area was affected by a cold front that generated partly cloudy conditions with slightly lower air temperatures, so that photochemical processes were less activated, resulting in less contribution to the increase in ozone. As the air temperature was still 3 °C or 5 °C higher than temperatures on March 26 and 29 when no windstorm occurred, photochemically produced ozone on that day was potentially much higher than on the other two days.

### 3.3 Effects of atmospheric circulation and atmospheric boundary layer – daytime

Figures 7, 8 and 9, respectively, show a plan view of wind vectors at 10 m, simulated by the LAS-V meteorological model at 1200 LST and 1800 LST on March 27, a vertical wind profile at the same times, and the same vertical profile showing wind speeds also at 1200 LST and 1800 LST on 27 March, during the windstorm. At 1200 LST, the simulated surface winds near Kangnung city consisted of two different wind regimes, namely, a synoptic scale south-westerly wind over the top of Mt. Teagwallyang and a meso-scale easterly sea breeze coming from the East Sea. The westerly wind moving downslope on the eastern side of the mountains could reach windstorm conditions with a maximum speed of 24 m s<sup>-1</sup>, bypassing the coastal city of Kangnung in a hydraulic jump motion, with

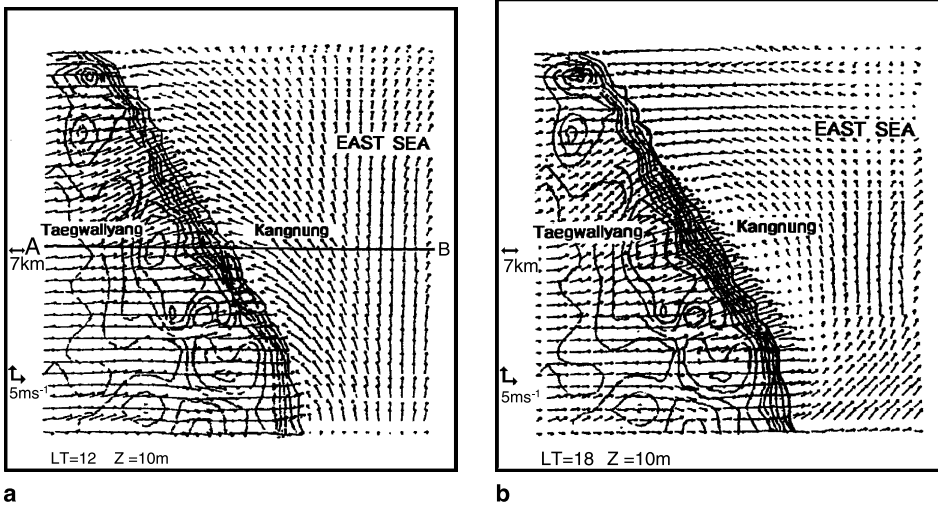


**Fig. 7.** Surface wind vectors ( $\text{m s}^{-1}$ ) at 10 m height above sea level near Kangnung city in the fine-mesh model domain on March 27, 1994 at, (a) 1200 LST and, (b) as in (a) except 1800 LST

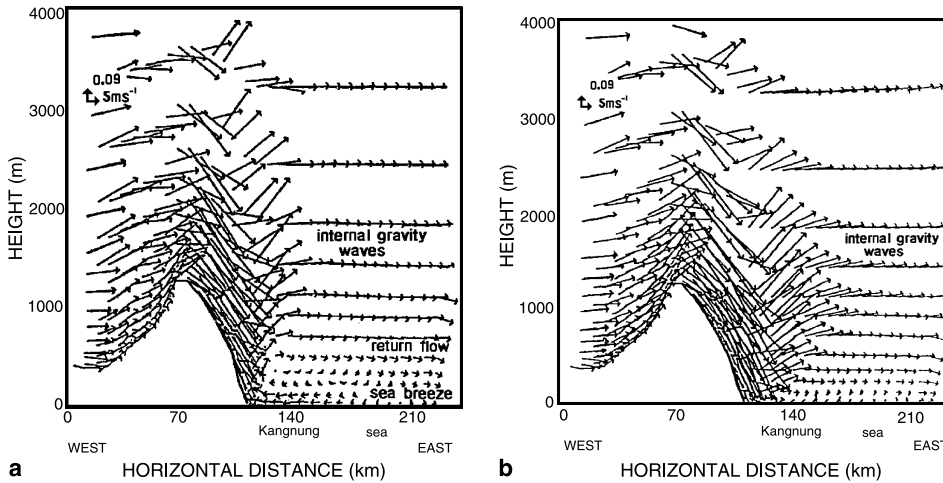


**Fig. 8.** Vertical wind profile ( $\text{m s}^{-1}$ ) on the line, A-B (Mt. Taegwallyang-Kangnung city- the East Sea) in Fig. 7a on March 27, 1994 at, (a) 1200 LST and, (b) as in (a) except 1800 LST

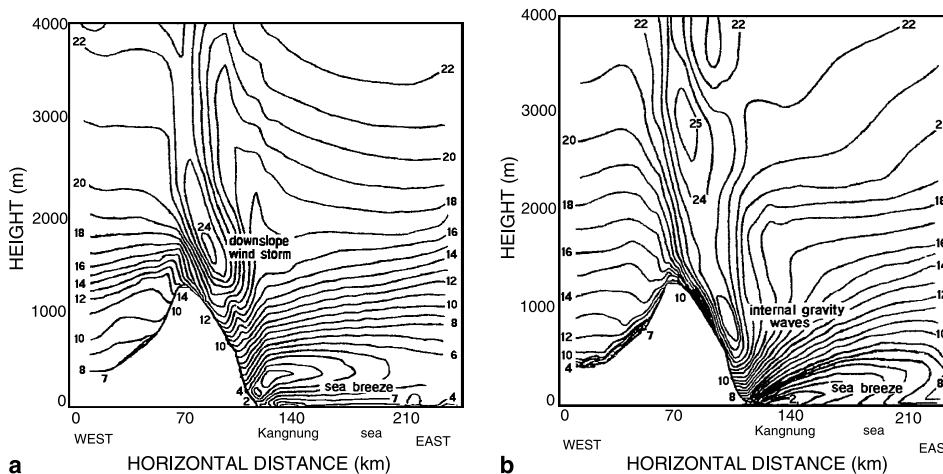


**Fig. 9.** As shown in Fig. 8, except for wind speed ( $\text{m s}^{-1}$ ) at, (a) 1200 LST and, (b) as in (a) except 1800 LST

ascent occurring over the East sea adjacent to the coast. The sea breeze at Kangnung city initially has a speed of  $7 \text{ m s}^{-1}$  and at the surface just on the lee side of the mountain it was  $2 \text{ m s}^{-1}$  in the convergent area created by the opposing westerly wind. The wind direction in the coastal region was easterly and south-easterly.

At 1800 LST (approximately sunset), the sea breeze circulation became smaller in horizontal extent, even though the surface wind was still easterly. This feature was attributed to the intrusion of a more intense westerly wind regime toward the coast, as the sea breeze weakened under reduced thermal forcing due to solar radiation. In this type of meteorological situation in the mountainous coastal plain near Kangnung city, the convective boundary layer (CBL) during daytime hours generally extends to a height of 1500 m above ground over the coast and upslope of the adjacent mountains further west (Choi, 1996; Choi and Kim, 1997).

In this study, strong westerly synoptic-scale winds blowing over the top of the mountains and down the eastern slopes are intensified into windstorm speeds during daytime hours. Thus, the westerly windstorm conditions strongly suppressed upslope winds, namely, the combined easterly sea breeze and valley wind on the eastern slopes, causing a decrease in thickness of the convective boundary layer by two thirds (about 700 m). The normal thickness of the CBL is approximately 1500 m in the absence of windstorm conditions. Thus, the main contribution to the high daytime concentrations of  $\text{O}_3$  may

be due to the increase in  $\text{O}_3$  from photochemical reactions that produce  $\text{O}_3$  from  $\text{NO}_x$ . Moreover, a further increase in  $\text{O}_3$  concentration should be caused by the resulting thinner than normal CBL. This is one of the most important mechanisms responsible for the occurrence of unusually high daytime ozone concentration.

Figure 10 shows the potential temperature deviation ( $\theta' = \theta - \Theta$ ), obtained by subtracting the mean potential temperature of the atmosphere in the model domain from the potential temperature at each level. Contours of potential temperature deviation have the same meaning as contours of potential temperature. The upper troposphere along the eastern slopes at 1200 LST was very stable, enabling subsidence of air from the upper layers toward the ground. This resulted in the development of downslope westerly winds along the eastern side of the mountains. The intensified downslope westerly winds experienced rapid upmotion in the form of a hydrologic jump over the sea adjacent to the coast. As air parcels descended from the upper levels of the troposphere over the eastern slopes, some of the ozone could have been transported down close to the surface, but might not reach the surface at the coast, due to the opposing easterly sea breeze (Fig. 9).

On the other hand, the air below 700 m in the thinner CBL of otherwise 1500 m in depth, was unstable due to the surface heating by daytime solar radiation. This heating induced the easterly sea breeze circulation. Furthermore, as there was an upper subsidence inversion layer near a

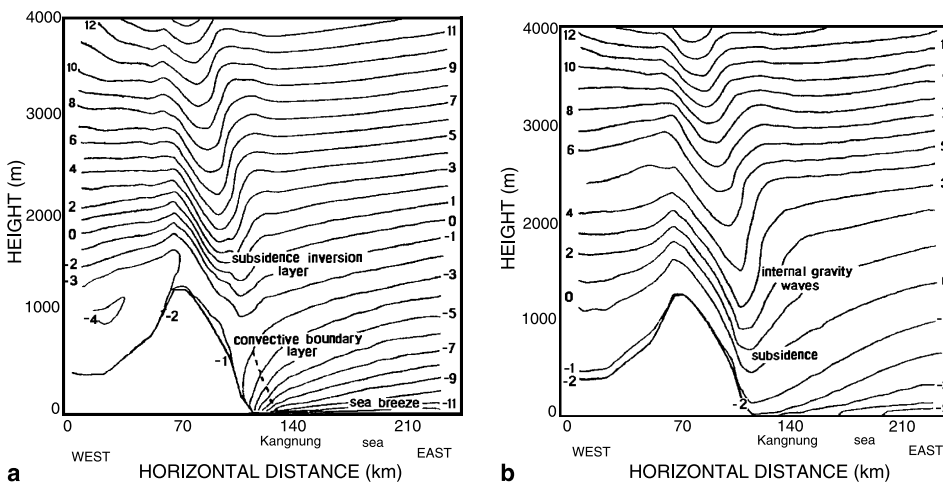


**Fig. 10.** As shown in Fig. 8, except for contours of potential temperature deviation ( $\theta' = \theta - \Theta$ ) at, (a) 1200 LST and, (b) as in (a) except 1800 LST



height of 700 m over the coast, the easterly sea breeze was able to undercut the strong westerly downslope winds through Kangnung city up to a height of approximately 400 m. Unstable marine air then returned seawards at upper levels. Surface ozone at Kangnung city that was within the CBL under the influence of the easterly sea breeze had a different origin from ozone near the top of the mountains on the westerly or upwind side.

Although the main contribution to the daytime high concentrations of  $O_3$  was due to the production of  $O_3$  by photochemical reactions involving  $NO_x$ , further increases in  $O_3$  concentration within the shallower than normal CBL are much more significant in explaining why the surface ozone concentration under windstorm conditions was almost twice as high as without windstorm conditions. In Figs. 2 and 3, hourly variations of both  $NO_2$  and  $NO$  on March 26, in the absence of windstorm conditions, showed similar patterns as on March 27 when windstorm conditions did occur. However, daytime surface ozone concentrations on March 27 were much higher than on March 26. This appears to be a very important mechanism for the occurrence of unusual daytime high ozone concentration in the mountainous coastal boundary layer.

At 1800 LST, which is close to sunset, the contours of potential temperature deviation on the lee side of the mountains (Fig. 10b), indicated much greater subsidence warming than at 1200 LST (Fig. 10a). The energy of the lee waves

(internal gravity waves) effectively propagated upwards and the wind increased to reach windstorm speeds. The centre of the windstorm descended along the eastern slope of the mountain close to the surface. The CBL was much thinner and the sea breeze circulation was much smaller in extent at this time than at 1200 LST. An upper level subsidence inversion layer apparently descended approximately half way down the eastern slopes of the mountains. In this situation, momentum transport of air masses can occur from upper levels of the troposphere toward the ground in the coastal region, as shown in Fig. 15.

Even if the production of  $O_3$  from  $NO_x$  through photochemical reaction processes decreased, the thinner than normal boundary layer appears to have contributed to the increase in the accumulated daytime ozone. As westerly windstorm conditions descended towards the surface of the coastal region, the CBL became shallower and the sea breeze circulation became weaker. Thus, vertical mixing of air masses, transported from the upper troposphere toward the surface, with air masses in the CBL associated with the sea breeze could occur, resulting in the enhancement of ozone concentration near the surface.

### 3.3 Effects of atmospheric circulation and boundary layer – nighttime

Next, the driving mechanisms responsible for the occurrence of high ozone concentration at night

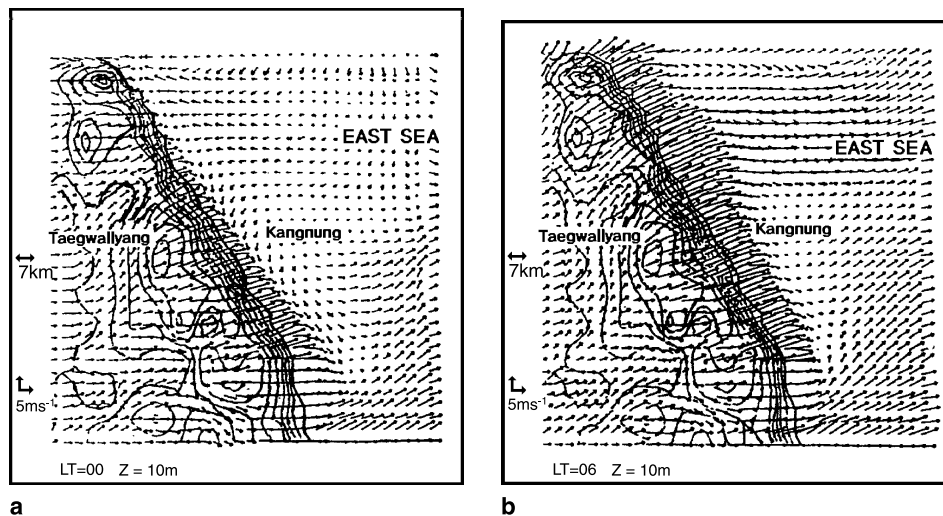


**Fig. 11.** Surface wind vectors ( $m s^{-1}$ ) at 10 m height over the sea surface near Kangnung city in the fine-mesh domain at, (a) 0000 LST, March 28, 1994 and, (b) as in (a) except at 0600 LST

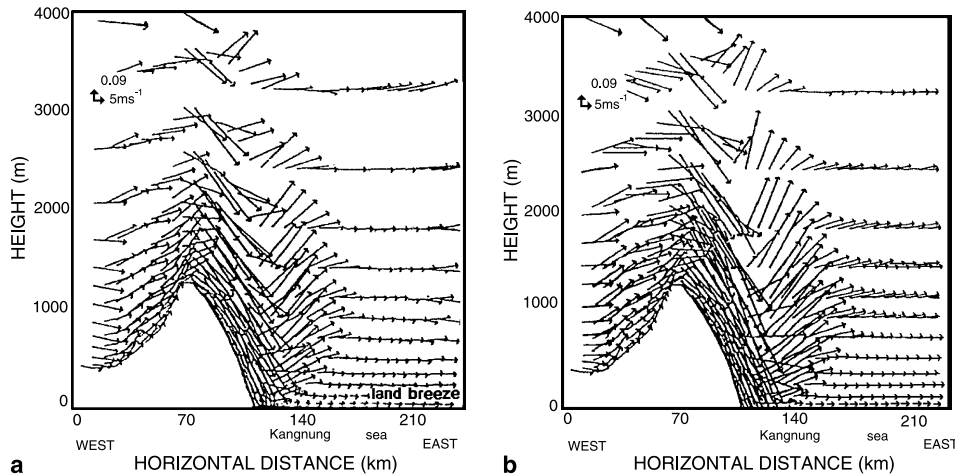


**Fig. 12.** Vertical wind profile ( $\text{m s}^{-1}$ ) on a line through Mt. Taegwallyang-Kangnung city- the East Sea in Fig. 11 at, (a) 0000 LST, March 28, 1994 and (b) as in (a) except at 0600 LST

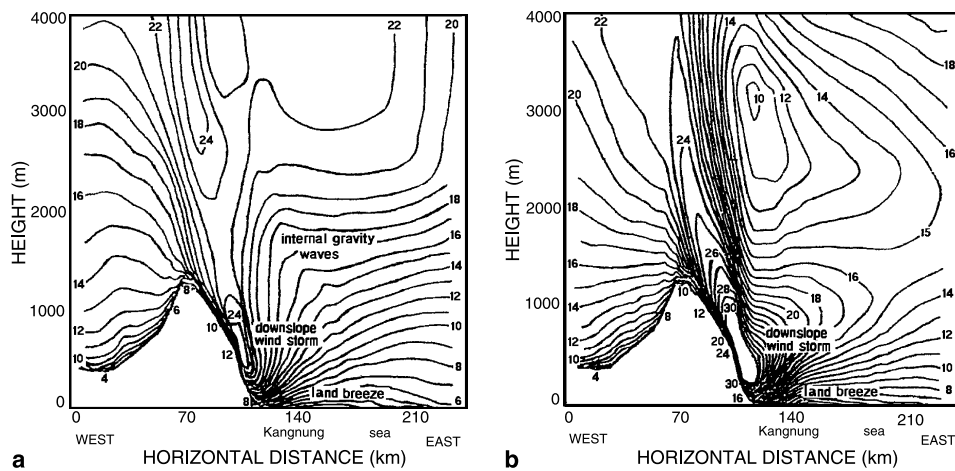


**Fig. 13a.** As shown in Fig. 12, except for wind speed at 0000 LST, and (b) at 0600 LST, March 28, 1994

are discussed. Figures 11, 12 and 13 show wind vectors at the surface, a vertical wind profile and wind speed, respectively, for nighttime hours at 0000 LST and 0600 LST on March 28, 1994. After sunset, at 1900 LST, March 27, there was no solar radiation at the surface. During the day strong westerly winds that were present along the mountain slope should be intensified by both the westerly downslope wind and the westerly land breeze directed from the inland basin toward the East Sea. The westerly land breeze occurs due to the different nocturnal cooling rates of the land and sea.

Thus, as the strongly enhanced westerly wind rapidly descended along the steep mountain slope, it reached windstorm strength with a maximum speed of  $30 \text{ m s}^{-1}$ . The wind speed at the

base of the eastern slope increased to a critical threshold and a hydraulic jump occurred near the surface at Kangnung city, ascending up to upper tropospheric levels over the sea. This resulted in a return flow and the generation of lee-side internal gravity waves. At that time, the observed surface wind speed at Kangnung city was  $10 \text{ m s}^{-1}$ . As indicated in the sequence of figures, the centre of the wind storm, which reached maximum wind speeds above  $28 \text{ m s}^{-1}$ , progressively descended towards the surface. At 0600 LST, just before sunrise and when a maximum speed of  $30 \text{ m s}^{-1}$  occurred, the core reached its lowest height of approximately 200 m above ground.

At this time, strong momentum transport of air from upper tropospheric levels directed toward the surface readily occurred and high ozone

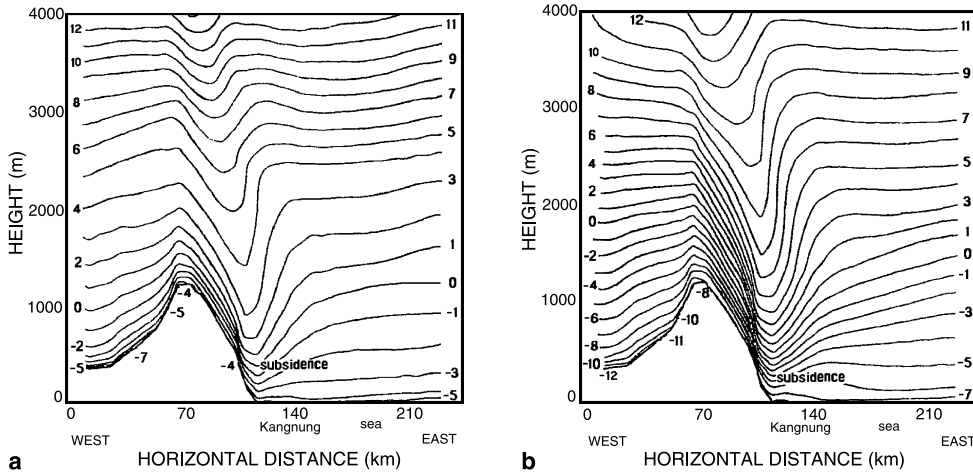


**Fig. 14a.** As shown in Fig. 12, except for potential temperature deviation lines ( $\theta' = \theta - \Theta$ ) at 0000 LST, and **(b)** 0600 LST, March 28, 1994

concentrations in the upper troposphere could easily be transported to the surface, enhancing the surface ozone concentration at night. On March 27, vertical profiles of wind speed indicate the possibility of momentum transport of air from a height of 10,000 m to the surface (Fig. 15). However, even if it meteorological events such as the occurrence of downslope windstorms can fully induce air parcels to descend to the surface, it is, at present, very difficult to estimate quantitatively how much upper level ozone would be

transported to the surface, since ozone data due to this process is not measured.

Consequently, the westerly winds increase to windstorm speed not only due to a topographical gradient and nocturnally produced land breeze (local effect), but also by momentum transfer from the strong upper tropospheric winds toward the surface near Kangnung city (synoptic scale effect). The wind storm intensity increases to a maximum speed of  $30 \text{ m s}^{-1}$  at 0600 LST, the next morning. On March 28, the wind pattern was similar to that on March 27. On March 29, after the end of the windstorm, winds increased to moderate strength again, similar to March 26, before the beginning of the storm, and a typical wind pattern controlled by only the sea-land breeze circulation was clearly observed in the coastal region. Thus, the surface ozone concentration, in the absence of windstorm conditions was not affected by the wind regime.

From 2100 LST to 0600 LST on both March 27 and March 28, the near surface night air was too stable due to strong nocturnal cooling of the surface. The potential temperature gradient increased along the slope and was larger than over the sea adjacent to the coast. Under the influence of a stable nocturnal boundary layer westerly downslope wind speeds can increase and be responsible for the maximum surface wind speed of  $28 \text{ m s}^{-1}$  until 0900 LST. At night, the downslope wind associated with the mountain-land breeze should be re-enforced locally to windstorm speeds along the lee-side of the

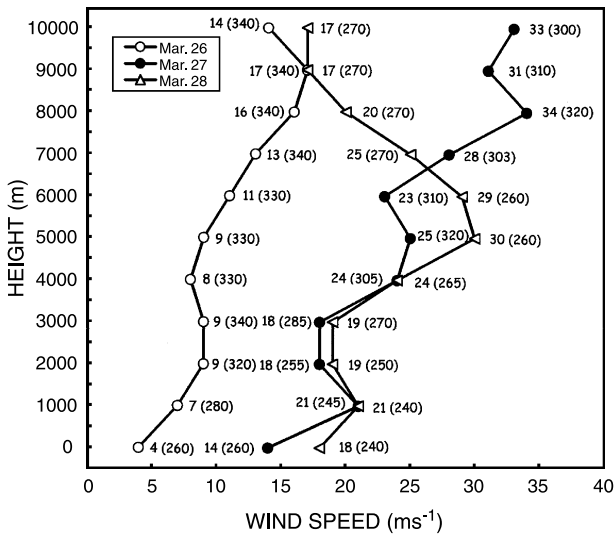


**Fig. 15.** Vertical wind profile ( $\text{m s}^{-1}$ ) from the surface to 10,000 m as measured by balloon at Korea Air Force Base in Kangnung city at 0900 LST for March 26, 27 and 28, 1994. ( ) denotes wind direction

mountain near Kangnung city, leading to an extremely shallow nocturnal surface inversion layer (NSIL). As the upper level subsidence inversion layer reaches the surface and combines with the nocturnal surface inversion, vertical mixing of air transported from the upper troposphere can occur with air near the surface.

### 3.4 Momentum transport from upper atmosphere

Figure 15 shows vertical wind profiles measured by balloon at the Korean Air Force Base at Kangnung at 0900 LST, March 26 through March 28 (no data for March 29). It clearly indicates momentum transport of air from the upper troposphere to the surface on March 27, which was here defined as a windstorm day. Kim et al (2002), Davis and Schuepbach (1994) and Moon et al (2002) emphasize that stratosphere-troposphere exchange is associated with weather conditions such as tropopause folding at the rear of an upper level jet streak. Such a vertical wind profile could induce air in the upper troposphere to descend toward the surface in the study area enabling ozone from the upper levels to be transported to the coastal surface, causing the enhancement of surface ozone concentration during the storm period.

On March 26, the wind speed at approximately a height of 10,000 m was relatively weak, as both the upper level and surface wind speed at the coast was also very weak. On March 28, it is very difficult to expect any momentum transfer from the upper troposphere toward the surface. When we expect momentum transport of air to occur from upper levels to lower levels, the wind speed gradually increases first in the low levels then in the upper levels. On that day, the wind increased from the surface to a height of 5000 m and then decreased between 5000 m and 10,000 m. The vertical momentum transport was confined only to March 27.

Thus, the higher nocturnal concentration of  $O_3$  mainly depended upon the decreased thickness of the NSIL and some  $O_3$  was transported by the momentum transfer from the upper troposphere (above 6 km) toward the surface, under the development of extreme windstorm conditions.

Even though the destruction of  $O_3$  occurred though the reaction of  $NO_x$  with  $O_3$ , a high con-

centration of ozone could be generated under the occurrence of windstorm conditions.

### 3.5 Advection from Wonju city

Further consideration was given to advection of  $O_3$  from an inland urban city, Wonju, which is located on the upwind side of the mountains and 100 km from Kangnung city. Figure 16 shows the hourly variation of wind speed at Wonju city. On March 26 and March 29, before and after the occurrence of the windstorm at Kangnung, the wind strength at Wonju was moderate during the day and very light at night. When windstorm conditions were present at Kangnung city on March 27 and March 28 the wind speed at Wonju city increased to 2 or 3  $m s^{-1}$  higher than in the absence of windstorm conditions at Kangnung city during daytime hours, namely, 4  $m s^{-1}$  to 6  $m s^{-1}$ . During nighttime hours, wind speeds either with or without the presence of a windstorm at Kangnung city, were very light (less than 2  $m s^{-1}$ ). As the wind speed generally increases during the day, due to thermally induced and topographically enhanced airflow in the basin, the wind speed is relatively higher during the day than at night.

In Fig. 17,  $O_3$  concentration at Wonju city indicated a maximum value in the afternoon and a minimum at night, regardless of the occur-

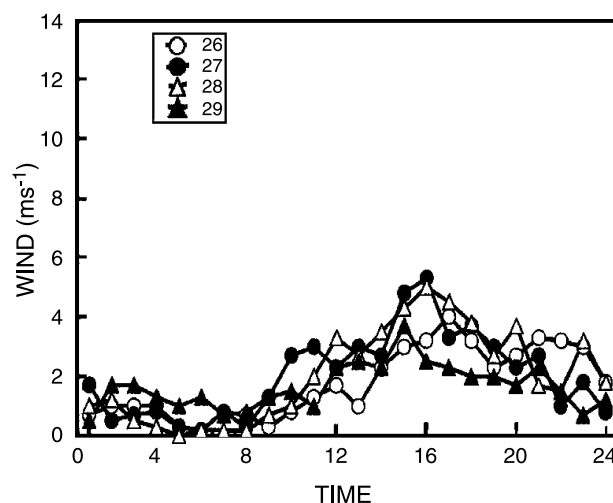


**Fig. 16.** Hourly concentration of wind speed ( $m s^{-1}$ ) from March 26 to March 29, 1994 at the inland city of Wonju, located on the upwind side of the mountains, and 100 km west of the coastal city of Kangnung

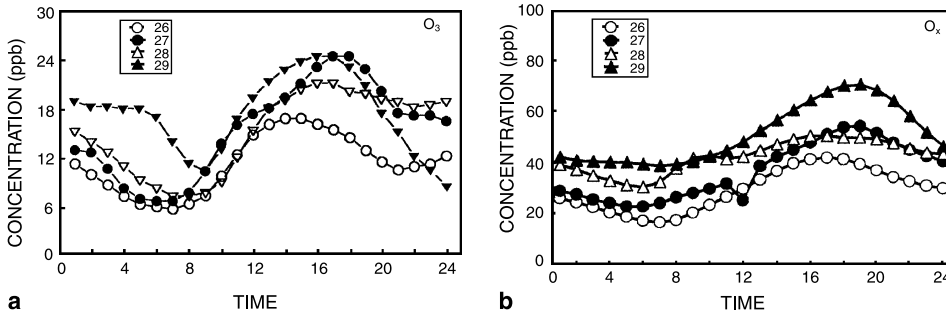


**Fig. 17a.** Hourly concentrations of O<sub>3</sub> (ppb), and **(b)** as in (a) except for O<sub>x</sub> (ppb), at Wonju city, from March 26 to March 29, 1994

rence of windstorm speeds at Kangnung city, even though Wonju city experiences moderate westerly winds. Ozone concentration at Wonju city on March 27 and March 28 under windstorm conditions was similar in magnitude to the concentration on March 29 and higher than the concentration on March 26, in the absence of windstorm conditions. Maximum surface O<sub>3</sub> concentration on March 26 was detected at 1600 LST.

Just after sunset (approximately 1800 LST), the concentration gradually decreased, until midnight. After midnight, ozone concentration rapidly decreased until 0600 LST (approximately sunrise). This diurnal tendency persisted until 0900 LST on March 29, at the time the windstorm ceased at Kangnung city. From approximately 2000 LST to mid-night, ozone concentrations for the windstorm period were about 7 ppb higher than for the non-storm period, but the concentration after mid-night was almost the same, regardless of the occurrence or not of a windstorm.

If we assume that these concentrations of ozone during the windstorm period could be transported from Wonju city to Kangnung city and the coast, they may partially act to the increase the nighttime ozone concentration at Kangnung. Figures 17 and 18 show hourly concentrations of O<sub>x</sub> and NO<sub>x</sub> at the inland city, Wonju (upwind side). Figure 19 also shows O<sub>x</sub> concentration at Kangnung (lee side). The distribution of O<sub>x</sub> concentration at the two cities was similar to that of NO<sub>x</sub>, and their maximum concentrations occurred in the afternoon. NO concentration at Wonju city was twice as high as NO<sub>2</sub> concentration, while NO concentration at

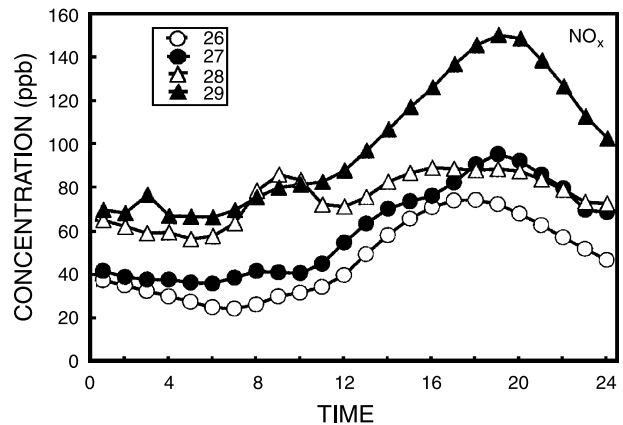


**Fig. 18.** Hourly concentration of NO<sub>x</sub> (ppb) at Wonju city from March 26 to March 29, 1994

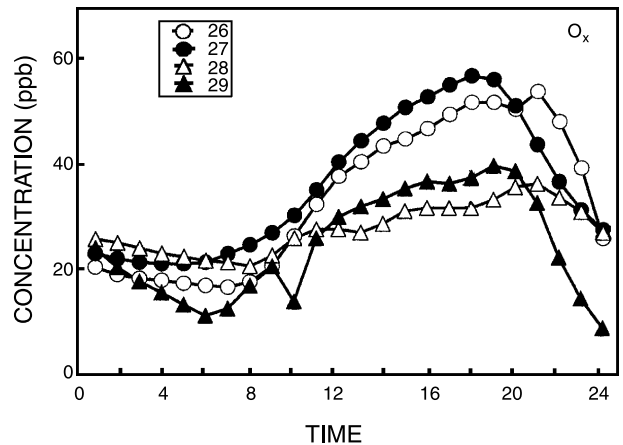


**Fig. 19.** Hourly concentration of O<sub>x</sub> (ppb) at Kangnung city from March 26 to March 29, 1994

Kangnung city was slightly lower than NO<sub>2</sub> concentration (Figs. 2 and 3). The concentration of NO, particularly at Kangnung, was very low

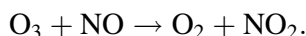
(ranging between 1 ppb and 34.3 ppb), while the concentration at Wonju was three times higher than the concentration at Kangnung. This implies that the emitted amount of NO at Wonju city was three times as high as at Kangnung.

Thus, NO<sub>x</sub> concentration with a maximum of 108 ppb at Wonju city was about twice the concentration at Kangnung. Therefore, under the influence of westerly winds, some NO on the upwind (western) side can be transported down-slope on the lee (eastern) side to Kangnung city. Although the advection of O<sub>3</sub> from Wonju city toward Kangnung city might not be enough to substantially increase O<sub>3</sub> concentration at Kangnung city continuously throughout the day, it still significant and should be considered.

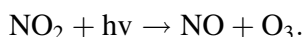
In an area without local emission sources such as Kangnung city, NO<sub>2</sub> concentration was much greater than ozone concentration. It may be important to consider the oxidant capacity,

$$O_x = NO_2 + O_3$$

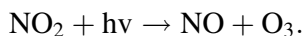
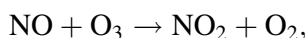
due to a fast reaction such as



Thus, O<sub>3</sub>, stored as NO<sub>2</sub>, will be released again by photolysis during the day, as follows:



Therefore, O<sub>x</sub> represents the natural O<sub>3</sub> background in the absence of NO<sub>x</sub> (= NO + NO<sub>2</sub>). In Figs. 19 and 3, the diurnal variations of O<sub>x</sub> and NO<sub>x</sub> at Kangnung city were similar, because of the rapid equilibrium state achieved between them in the presence of sunlight, namely,



This has implications for the transport process into remote rural areas of aged chemical air masses. Very small ozone concentrations were found in Germany (Kley, 1992; Moller, 2001), by comparing ozone concentration at Cologne city with that in a rural forest area about 30 km away. In that study, small values of O<sub>x</sub>, NO<sub>2</sub> and O<sub>3</sub> (35 ppb, 20 ppb and 15 ppb), respectively, were detected in Cologne city compared to similar values of 35 ppb, 5 ppb and 30 ppb in the forested area.

## 4. Conclusions

During windstorm conditions in southern Korea, high O<sub>3</sub> concentration during the day on the lee side of the mountainous coastal region is mainly due to processes involving photochemical reactions of NO<sub>x</sub> into O<sub>3</sub> and a reduction in the thickness of the convective boundary layer. At night, although O<sub>3</sub> should be destroyed in the absence of solar radiation, its concentration still increases within the very shallow nocturnal surface inversion layer, as it is transported towards the surface by momentum transfer in the windstorm conditions. Some of the ozone being transported from the upper troposphere toward the surface might contribute to the increase in ozone concentration. Furthermore, advection of ozone from the inland city of Wonju on the upwind side toward the coastal city of Kangnung on the downwind side, may also partially act to increase the surface ozone concentration.

## Acknowledgements

This research is partially supported by a grant-in-aid for scientific research project of Dual Use Technology-“Virtual Marine Environmental Analysis Technology for Systematic Operation from Ministry of Science and Technology (MOST) in 1999–2000: Verification and Prediction of Marine Wind through Marine Observation”. The author would like to thank Dr. Detlev Moller, Brandenburg Technical University for helpful comments.

## References

- Austin JF, Midgley RP (1994) The climatology of the jet stream and stratospheric intrusion of ozone over Japan. *Atmos Environ* 28A: 39–52
- Baird C (1995) *Environmental chemistry*. Freeman
- Boybeyi Z (2000) *Mesoscale atmospheric dispersion*. Southampton: WIT Press, pp 315–322
- Choi H (1996) Numerical modeling for air flows in the eastern mountainous coastal seas of Korea. *La Mer* 34: 133–148
- Choi H, Kim J (1997) Three-dimensional numerical prediction on the evolution of nocturnal thermal high (tropical night) in a basin. *Korean J Geophys Res* 25: 57–81
- Cooper OR, Moody JL, Davenport JC, Oltmans SJ, Johnson BJ, Chen X, Shepson PB, Merrill JT (1998) Influence of springtime weather systems on vertical ozone distributions over three North American sites. *J Geophys Res* 103: 22001–22013
- Davies TD, Schuepbach E (1994) Episode of high ozone concentration at the surface resulting from transport down from the upper tropospheric/lower stratosphere. A review and case studies. *Atmos Environ* 28: 53–68

- Evans G, Finkelstein P, Martin B, Possiel N, Graves M (1983) Ozone measurements from a network of remote sites. *J Air Pollut Cont Ass* 33: 291–296
- Girdziene R (1991) Surface ozone measurements in Lithuania. *Atmos Environ* 25: 1791–1794
- Hales J (1996) Scientific background for AMS policy statement on atmospheric ozone. *Bull Am Meteor Soc* 77: 1249–1253
- Hobbs PV (2000) Introduction to atmospheric chemistry. Cambridge: Cambridge University Press, pp 143–163
- Jacob DJ (1999) Introduction to atmospheric chemistry. Chichester: Princeton University Press, pp 143–163
- Kim YK, Lee HW, Park JK, Moon YS (2002) The stratosphere-troposphere exchange of ozone and aerosols over Korea. *Atmos Environ* 36: 449–463
- Kimura F (1983) A numerical simulation of local winds and photochemical air pollution (1): two-dimensional land and sea breeze. *J Meteor Soc Japan* 61: 862–878
- Kondratyev KY, Varotsos C (2000) Atmospheric ozone variability: Implications for climate change, human health and eco-system. Berlin: Springer, 617 pp
- Mckee DJ (1994) Tropospheric ozone. Boca Raton, FL: CRC Press, 333 pp
- Moller D (2001) Photooxidation capacity. Workshop on Local and Regional Contribution to Air Pollution and Local Radiative Balance in Asian Developing Countries, Guangzhou, China, September 27–30
- Moon YS, Kim YK, Strong K, Kim SH, Lim YK, Oh IB, Song SK (2002) Surface ozone episode due to stratosphere-troposphere exchange and free troposphere-boundary layer exchange in Busan during Asian dust events. *J Environ Sci* 11: 419–437
- NFRADA (1994) Analyzed NOAA satellite picture on the sea surface temperature. National Fisheries Research and Development Agency
- Pazenny A, Brasseur G (1997) Tropospheric ozone: An emphasis on IGAC Research. *Global Change Newsletter* N30: 2–10
- Seinfeld JH, Pandis SN (1998) Atmospheric chemistry and physics: From air pollution to climate change. New York: Wiley, 1326 pp
- Takahashi S (1997) Manual of LAS model revised by Dr. J. Sato, 50 pp
- WREA (1994) Measured data at Kangnung city in 1994, 100 pp

Author's address: H. Choi, Environmental Science Center, Peking University, Beijing 100781, P.R. of China (E-mail: du8392@hanmail.net)